# Inrush Current Testing

Erik K. Saathoff†, Zachary J. Pitcher†, Steven R. Shaw‡, Steven B. Leeb†

†Department of Electrical Engineering and Computer Science
Massachusetts Institute of Technology, Cambridge, MA, USA

‡Department of Electrical and Computer Engineering
Montana State University, Bozeman, MT, USA

***Abstract*—Inrush current testing is used for a variety of purposes including sizing fuses and carrying out power supply performance verification. Effective, accurate inrush testing can do more, including enabling power quality measurements and generating exemplars for machine-learning systems monitoring the power line. Some off-the-shelf AC power supplies offer capabilities for controlled inrush testing, but control dynamics and power limitations affect the shape, peak, and time constants of the results. Also, AC power sources obscure details of the grid connection to a load. To provide more accurate and relevant results, a phase-controlled switch is demonstrated as an alternative that can be used *in situ*. Established or existing line impedance is automatically included for realistic measurements. This paper reviews the design and performance of a proposed phase-controlled switch, and also reviews application of the measured data for line impedance estimation.**

## I. Introduction

Many loads, such as lights, induction motors, and power supplies, can draw large inrush currents. A load's inrush current is an important performance characteristic that affects the grid [1]–[4] and protection elements [5]. In some cases, these currents may exceed ten times the steady-state peak level. Transient behavior also provides valuable information for load identification in nonintrusive power system monitors since transient patterns serve as fingerprints for load identification and diagnostics [6]–[9]. Since transients vary with load activation times and the associated phase of the utility, an orderly system for collecting transient information at different points in the line cycle can provide an efficient data set for monitoring, diagnostics, and applications of machine-learning to power systems. Transient information can also be used for sizing protection gear and examining power quality interactions between equipment sharing a grid service. This paper will demonstrate the application of transient information for estimating line impedance.

Ideally, a transient testing device offers the possibility of examining load transients collected at different turn-on times and phases of the electric utility for both single- and three-phase loads. Inrush data collected over a range of phase angles permits determination of worst-case peak currents, as well as a range of possible transient variations for each load. Test equipment companies [10], [11] offer AC power supplies that perform transient testing by turning on loads at selectable phase angles. These tests may be excellent for loads with limited inrush currents, e.g., with an NTC or inductive input impedance. However, loads with significant inrush will strain or exceed the energy storage and feedback loop limitations of the AC supply. Also, load transients depend on the utility connection in real-life, a detail that may be eliminated by a power supply. This paper proposes test hardware that permits *in situ* experimentation, which enables testing that accounts for the effects of source and line impedance.

To preserve the effects of source and line impedance upstream from a load, a three-phase phase-controlled switch (Fig. 1), spliced into the electrical connection, performs the inrush sweep over a range of turn-on angles. The switch introduces small parasitics to prevent distorting the current. The transient test results provide realistic information on how a load will interact with its power source in practice. The approach described here provides "worst-case" transient test capabilities over a range of turn-on phase angles, thus providing exemplar waveforms that represent a range of practical behavior.


Fig. 1: Complete load switch in its enclosure.

This paper first reviews the proposed transient tester, which is then used to examine the challenges of using conventional AC power supplies when performing inrush current testing. The effects of changing line impedance are also shown. To show other applications of the phase-controlled switch, the procedure for extracting the values of an $R-L$ line impedance model will be shown.

This work was supported by The Grainger Foundation and by the Cooperative Agreement between the Masdar Institute of Science and Technology (Masdar Institute), Abu Dhabi, UAE and the Massachusetts Institute of Technology (MIT), Cambridge, MA, USA - Reference 02/MI/MIT/CP/11/07633/GEN/G/00.

978-1-7281-4829-8/20/$31.00 ©2020 IEEE

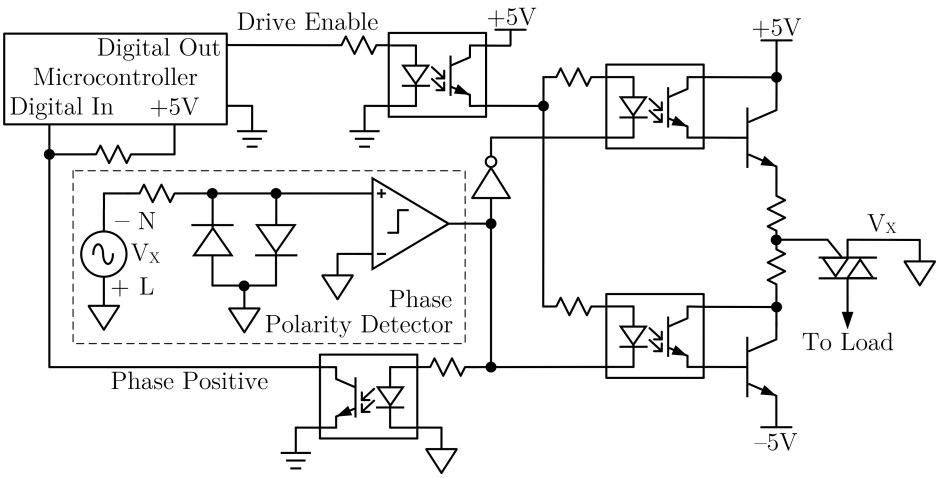


Fig. 2: Single-phase view of the driver, TRIAC, and phase polarity detector.

## II. Transient Test Hardware

For simplicity, the proposed phase-controlled switch is implemented with TRIACs. Fig. 3 shows the schematic of the tester. Since the TRIACs are spliced into the line connection, the source and line impedance feeding the load are preserved. The power devices introduce some non-idealities due to voltage drop, incremental resistance, parasitic series inductance, and gate drive dynamics. The approach demonstrated here can be extended to other semiconductor switch arrangements including MOSFETs and GaN FETs, permitting different constructions that can be tailored to minimize parasitic effects. Other semiconductor switches can provide additional test behavior, including multiple turn-on and turn-off events within a line cycle. The stochastic effects of real mechanical switches could also be emulated with more complex semiconductor devices. Among other uses, the intention of the proposed phase-controlled switch is to repeatably generate a range of inrush transients as a function of turn-on angle while including the effects of line and source impedance.

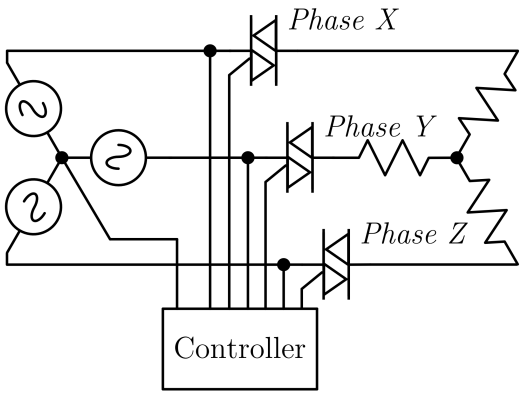


Fig. 3: Three-phase diagram of the source, switch, and load.

### A. Hardware Design

The switch rating is 30 A and 208 V (line-to-line), reflecting the voltage and current limitations of typical three-phase receptacles. To handle this current, Q6040K5TP alternistor TRIACs were chosen. Also, the TRIAC selected is rated for 400 A pulsed current, which improves the robustness of the switch when exposed to high currents. This switch choice introduces a small voltage drop. Other semiconductor devices, employed in the proposed circuit with rearrangements of the gate drive, can reduce this drop. With appropriate heat-sinking and a fan, the case-to-ambient thermal resistance is approximately 0.9 °C/W per device, while the junction-to-case thermal resistance is 0.97 °C/W. The junction-to-ambient thermal resistance is sufficiently low to allow continuous operation at full current, where each device dissipates 30 W.

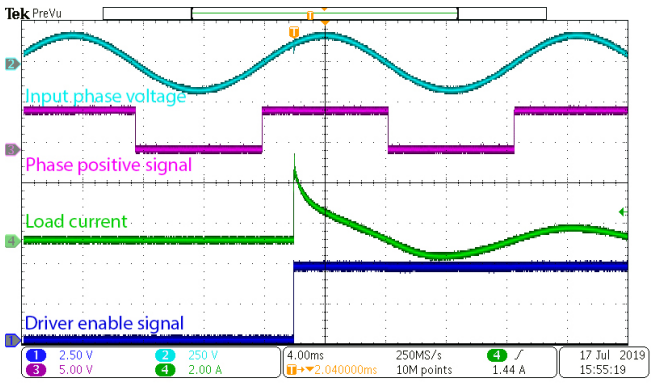


Fig. 4: Waveforms showing the operation of the phase-controlled switch for a 45° turn-on.

Since the equipment is intended for both single- and three-phase loads, wye input power is needed. The neutral of the input voltage source is required for operation of the phase polarity detector as shown in Fig. 2. The switch can handle either wye or delta loads. The difference between the line and

neutral voltage is sent to a bipolar comparator protected with low-capacitance diodes. The binary output is sent to a Cypress PSoC 5LP microcontroller (MCU) that uses a positive-edge-triggered timer to perform the phase control. The MCU also provides a convenient terminal interface and a timer resolution of 250 ns. The MCU monitors each TRIAC's temperature, controls fan speed, and can perform thermal shutdown if necessary. A "drive enable" signal is generated by the MCU and feeds the driver circuit for the TRIAC.

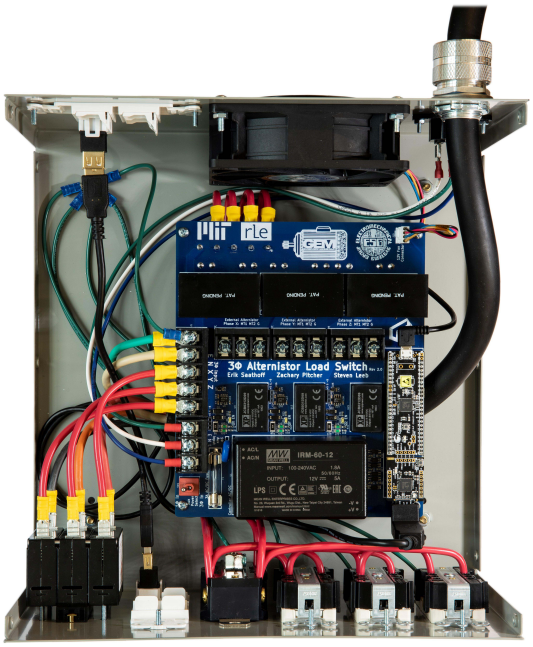


Fig. 5: Inside view of the assembled equipment.

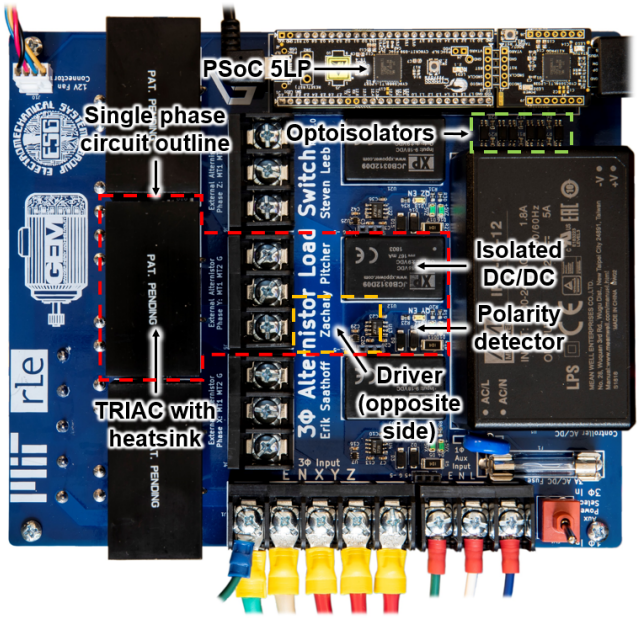


Fig. 6: Annotated view of the PCB.

Each phase has its own floating ground with an isolated DC-DC converter that generates bipolar voltage for the comparator and TRIAC driver. The polarity detector chooses the polarity of voltage applied to TRIAC gate and the drive enable signal is used to switch on the driver's output, which in turn turns on the switch. All circuitry between the MCU and driver circuit is sent through optocouplers for operator safety. Fig. 4 shows the relevant signals for a 45° turn-on angle. The "phase positive" signal switches as the line voltage goes negative and positive. In this example, the "driver enable" signal goes high 45° after one of the positive edges of the input signal, and the load current transient begins simultaneously. Figures 5 and 6 show the prototype hardware.

## III. Inrush Testing: Sources of Distortion

In general, the impedance of an electrical source affects the transient and steady-state response of a load. Performing an inrush test without regard to the system implementation can result in waveforms with significantly different characteristics from those found in practical use. In some cases, these effects are minimal and can be ignored. However, for loads with large inrush transients, the choice of source and line have dramatic effects on the results. This section demonstrates these effects and illustrates how the prototype can provide satisfactory test data for reflecting realistic load and grid performance.

### A. Source Effects

Inrush testing is commonly performed in the lab with an AC power supply that provides relatively low source impedance and controllable turn-on time. This method has the advantage of providing ideal sine waves of voltage, and decoupling the measurement from the electric utility. These supplies can produce results that are not significantly different from those captured with real grid connections when the power supply rating and bandwidth are not challenged substantially by the load requirements. For instance, a high impedance resistive load will have minimal interaction with the output filter and feedback control of a typical AC power supply. A transient from a commercial AC power source is shown in Fig. 7 for a wire-wound 155 Ω resistor connected to the line at 90°. Transients collected using both the power supply and the electric utility directly as sources are shown. Here, an Agilent 6834B configured for single-phase output, 120 $V_{RMS}$, and 30 $A_{RMS}$ current limit is used. This configuration will be used in other tests presented in this paper of the commercial AC power source.

The resulting transient shows that both the AC source and electric utility produce similar results for this load. The very fast current rise time of this load does create some oscillations in the power supply's feedback loop, but the shape of the current is reasonably preserved in both cases. Both sources provide an almost perfect match after only 50 $\mu$s.

Unfortunately, many loads make transient demands that challenge the capabilities on an AC power supply. An incandescent lamp load provides an illustrative example of the potential shortcomings of using an AC source. This type of

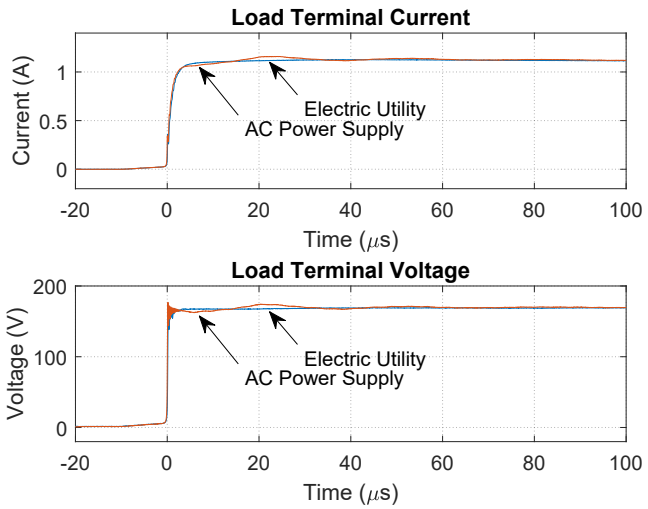


Fig. 7: Voltage and current waveforms for a 155 Ω resistor turn-on using either an AC power supply or the electric utility as the source.

load will have a steady-state power demand far below the rating of the AC power supply. However, the lamp transient peak current demand is not. The worst-case current peak is observed at the peak of the line voltage, i.e., a phase angle of 90°.

The resulting waveform in Fig. 8 shows a drastic drop in the line voltage generated by the commercial AC source during the initial 25 $\mu s$ of the transient. In contrast, the proposed AC transient tester avoids introducing distortions of the load behavior. Specifically, the resulting currents differ greatly between the two power sources at the beginning of the inrush current transient. Eventually, the waveforms are similar when the load demand stabilizes and the commercial AC source "catches up" to the load demand. Other types of loads, particularly ones with grid-connected power electronics, could generate a series of high $\frac{di}{dt}$ steps which would dramatically worsen the artifacts introduced by the commercial AC source. The proposed hardware, in combination with a practical electrical source, is necessary to provide more realistic results.

### *B. Line Impedance Effects*

Performing inrush testing using a lab's electric utility will remove some of the distortion caused by an AC power supply, but the line impedance will generally be different from field connections on the grid. Line impedance, as shown in Fig. 9, lowers the ability to quickly draw large currents from the source and will therefore impact inrush current testing. Additional line inductance will have the largest impact during high $\frac{di}{dt}$ steps and will significantly blunt high speed transients. Additional resistance will decrease the overall magnitude of the transient. To demonstrate this effect, a 100 ft single-phase utility cable, placed upstream of the phase-controlled switch, is added in the following experiments with the electric utility. The same incandescent lamp is used once again at a 90° turn-on angle to create the most apparent interaction with the line inductance.

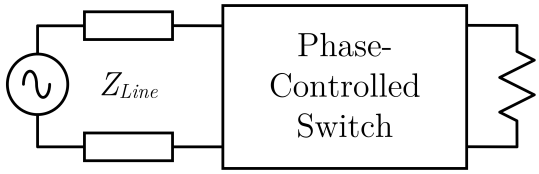


Fig. 9: Model of the source connection as a Thevenin voltage source with series impedance elements.

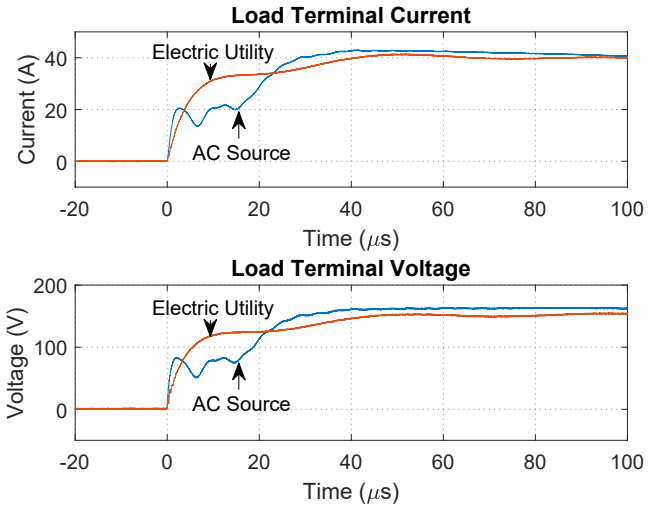


Fig. 8: Voltage and current waveforms for a 250 W incandescent lamp turn-on using either an AC power supply or the electric utility as the source.

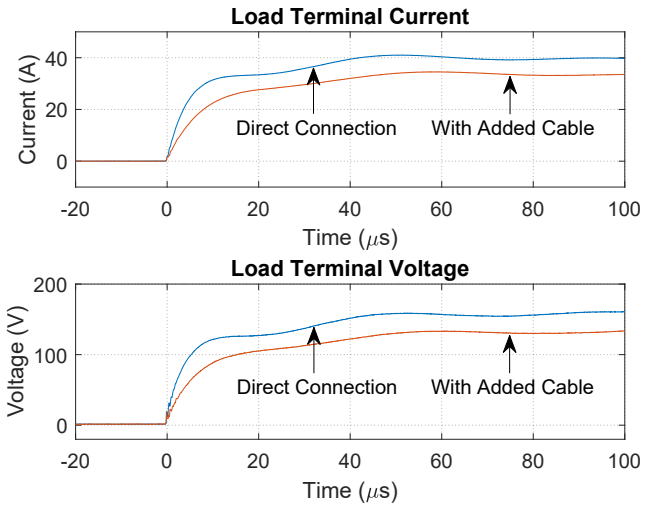


Fig. 10: Voltage and current waveforms for a 250 W incandescent lamp turn-on with or without added line impedance using the electric utility as a source.

Fig. 10 shows the turn-on transient both with and without the single-phase utility cable placed between the switch and the electric utility. The voltage and current delivered to the load is affected by the additional line impedance. Oscillations are slower, the initial current slew rate is reduced, and the peak inrush current is smaller with increased line impedance.

To include the effects of line impedance observed in the field, a line impedance network may be used in inrush current testing. Determining the arrangement and values of components for an accurate artificial network is complicated. Using a simplified line model of an inductor and resistor is adequate for modeling the utility in many cases, but does not necessarily capture load dynamics. For example, the voltage oscillations in Fig. 10 imply the presence of some line or load capacitance. Recreating the impedance involves choosing a complicated model that must be matched to the measured data. Instead, we propose that the testing is performed *in situ* in the electrical environment of interest using the load of interest to generate realistic data with less opportunity for modeling error.

## IV. Line Impedance Estimation

A useful application and demonstration of the phase-controlled switch is for generating data for line impedance estimation. Reference [12] presents a technique to determine the impedance of the electrical utility by connecting a capacitor to the line at a fixed point in the line cycle. Each test provides information on the apparent inductance and resistance. The resulting model is used to predict line voltage distortions caused by other current transients. References [13], [14] expand on this technique with a programmable capacitor to generate different oscillation frequencies. This approach creates a sweep of test frequencies for estimating the frequency dependent resistance of the utility wire.

The phase-controlled switch adds a new degree of flexibility in line impedance testing. The test load for line impedance estimation can still be a capacitor, with a selectable value of capacitance. The phase-controlled switch permits activation at an arbitrary point in the line cycle to allow for a selectable or variable level of transient current, providing additional data for system identification and also for limiting or expanding the test range on the utility. The switch can perform three-phase testing with a delta-connected capacitor to perform line impedance parameter extraction even in the absence of a neutral wire connection. Other loads, even typical utility or customer loads, can be used to perform similar types of line impedance analysis. The next section illustrates an application of the three-phase switch for line impedance estimation.

### A. System Identification

Line impedance might be modeled as a series $R-L$ circuit. The resistance and inductance can be extracted from measurements of suitably information rich voltage and current waveforms from the $R-L$ circuit. Fig. 11 shows a single-phase utility connection characterized by resistance $R$ and inductance $L$. The model voltage source is time shift invariant. That is, in practice, the utility voltage is assumed quasi-static for several line cycles to permit testing. Multiple samples may be taken and outliers discarded if conditions in the circuit or utility operation change.

To estimate line impedance, a cycle of the utility waveform is sampled and saved as a reference. In the immediate next cycle, the phase-controlled switch connects a load to the utility connection as shown in Fig. 11. The voltage $v$ and current $i$ are again sampled during the transient test. Subtracting the pre-transient cycle data from the transient cycle data isolates the behavior of the system due to the load transient from the background or "carrier frequency" operation of the utility.

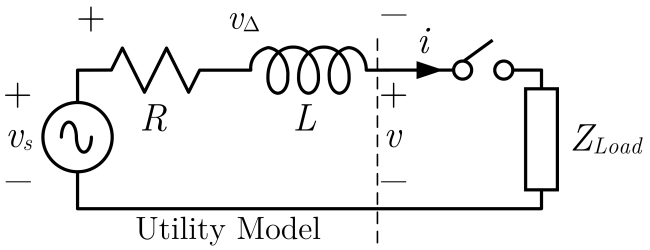


Fig. 11: Circuit model for the line impedance estimation.

This circuit is described by the KVL relationship:

$$v_s(t) - v(t) = v_\Delta(t) = (R + Lp)i(t) \tag{1}$$

where $p$ is the differential time operator. Measurements of voltage, current, and the derivative of current could be used to set up a least-squares tableau in order to solve for the desired parameters $R$ and $L$. This approach requires differentiation of an experimental waveform, and becomes more challenging and noise-prone as higher-order derivatives are computed for more complex systems. A state-variable filter or "lambda method" avoids the need to compute derivatives for the estimation problem.

Equation 2 defines the lambda operator [13]. This operator, when acting on a signal, computes the response of a first-order low-pass filter with time constant $\tau$ acting on the signal.

$$\lambda = \frac{1}{1 + p\tau} \tag{2}$$

The differential time operator $p$ can therefore be expressed as:

$$p = \frac{1 - \lambda}{\lambda\tau} \tag{3}$$

Substituting Eq. 3 into Eq. 1 gives:

$$\tau[\lambda v_\Delta](t)\frac{1}{L} - \tau[\lambda i](t)(\frac{R}{L} - \frac{1}{\tau}) = i(t) \tag{4}$$

where the terms in brackets give the result of the $\lambda$ operator acting on either the voltage drop or terminal current. This equation is solvable in principle with just two data points, but solving an over-constrained system with least squares provides a more reliable and noise resistant parameter estimation. The estimation uses only the input terminal voltage and current into the phase-controlled switch. The technique does not depend

on the parasitics of the switch, nor the characteristics of the chosen load.

The $\lambda$ operator acts on the array of $N$ voltage and current samples and the results are placed in the first matrix on the left of Eq. 5. The raw current samples are placed in the right side column vector. The equation shifts notation to refer to the indices of $\lambda$ filtered sample vectors. Since $\lambda$ is a continuous time operator, it is important to use finely sampled data to reduce the time quantization error. Solving this matrix equation by the least-squares approach gives estimates for the line inductance and resistance. The effects of noise in this technique are discussed in [15].

$$\begin{bmatrix} \tau[\lambda v_\Delta](1) & -\tau[\lambda i](1) \\ \tau[\lambda v_\Delta](2) & -\tau[\lambda i](2) \\ \vdots & \vdots \\ \tau[\lambda v_\Delta](N) & -\tau[\lambda i](N) \end{bmatrix} \begin{bmatrix} \widehat{\beta_1} \\ \widehat{\beta_2} \end{bmatrix} = \begin{bmatrix} i(1) \\ i(2) \\ \vdots \\ i(N) \end{bmatrix} \tag{5}$$

$$\widehat{\beta_1} = \frac{\widehat{1}}{L} \qquad \widehat{\beta_2} = \widehat{\frac{R}{L} - \frac{1}{\tau}}$$

### B. Experimental Results

To demonstrate the "lambda method" line impedance estimation technique and the utility of the phase-controlled switch, the impedance of a 100 ft section of single-phase utility cable is estimated. In these experiments, the phase-controlled switch connects a 250 W incandescent lamp to a utility connection at a variety of different phase angles, with and without an extended section of utility wiring upstream from the switch. The testing is carried out over a long time period so that the load cools completely between tests. Specifically, the load is off for three minutes between tests. The lamp is switched on for approximately 50 ms to minimize the thermal energy retained by the lamp. This procedure ensures that the filament is in thermal equilibrium with the environment at the start of each test.

Multiple tests are run at each phase angle to check for consistency. One test is performed at each of the desired phase angles. The sweep of phase angle tests is repeated to build a full data set. This protocol distributes the effects of drift across each phase angle's associated data.

For each set of waveform data captured, a section with the length of one full line cycle is used for computation with Eq. 5. The preceding cycle is used as the exemplar of the source voltage, which is used to find the transient voltage drop over the line impedance. In this example, $\tau$ is set at 1 $\mu$s.

The results of the inductance estimation are shown in Fig. 12 (a) for estimates with and without the single-phase utility cable. In the range of 40° to 140° voltage phase angle, the estimates are similar, and the range of values at each angle has a low variance. The difference between the two inductance estimates represents how much inductance the single-phase utility cable adds and is shown in Fig. 12 (b). The flat line at 20.33 $\mu$H shows the actual inductance of the added utility cable measured with an LCR meter. The match between the estimate and the real value demonstrates the effectiveness of this approach. Note that as the test phase angle approaches integer multiples of 180°, i.e., as the turn-on occurs closer to a voltage zero crossing, the variance increases and the average value drifts. Excitation is relatively low at these phase angles, and noise dominates the system identification problem. A practical application of the line impedance estimator would avoid these test phase angles to ensure a reliable data set.

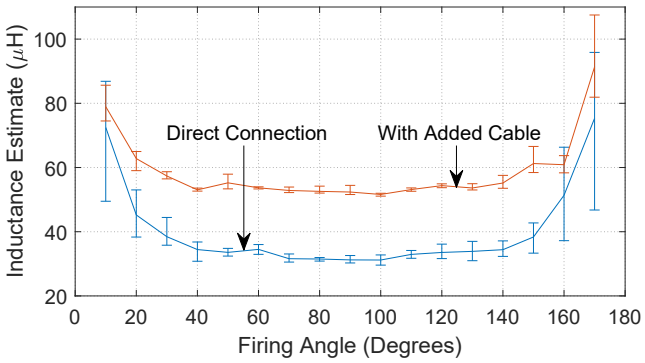


Fig. 12: (a) Average line inductance estimates for various turn-on angles with or without an added single-phase utility cable with the range of values from five tests shown. (b) Average line inductance of the utility cable for various turn-on angles.

Fig. 13 (a) shows resistance estimates with and without the added single-phase utility cable. Here, the variance in the resistance values remains consistent over the entire range of firing angles and the averages are roughly consistent. The difference between the estimates with and without the utility cable closely matches the impedance analyzer estimate of the cable as shown in Fig. 13 (b). The line plotted at 941 m$\Omega$ is the DC resistance of the wire. Of course, resistance is actually a function of frequency due to skin effect, but the resistance found on an LCR meter for this section of single-phase utility cable does not change significantly until the frequency exceeds 10 kHz; the resistance increases by around 1% at 10 kHz and by almost 20% at 50 kHz. Once again, excellent matching is achieved.

To achieve these results, it is necessary to ensure that the differential voltage probe and current clamp have their ratio carefully calibrated, and that the current clamp be calibrated

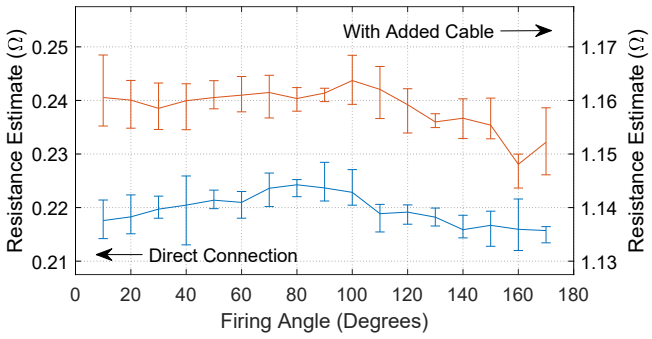


(a)

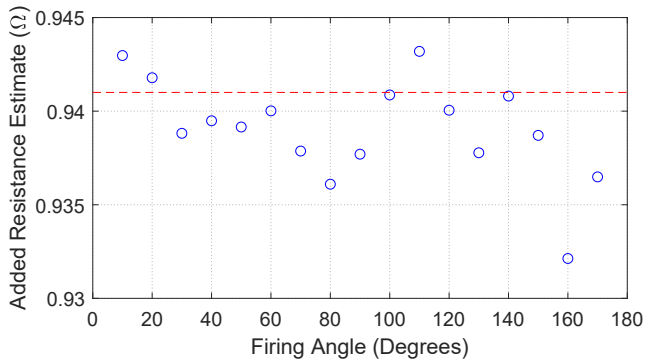


(b)

Fig. 13: (a) Average line resistance estimates for various turn-on angles with or without an single-phase utility cable with the range of values from five tests shown. (b) Average line resistance of the utility cable for various turn-on angles.

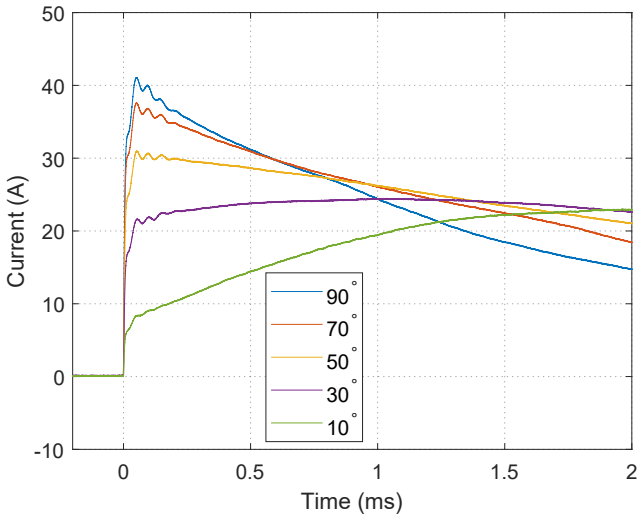


Fig. 14: Inrush currents observed at various turn-on angles.

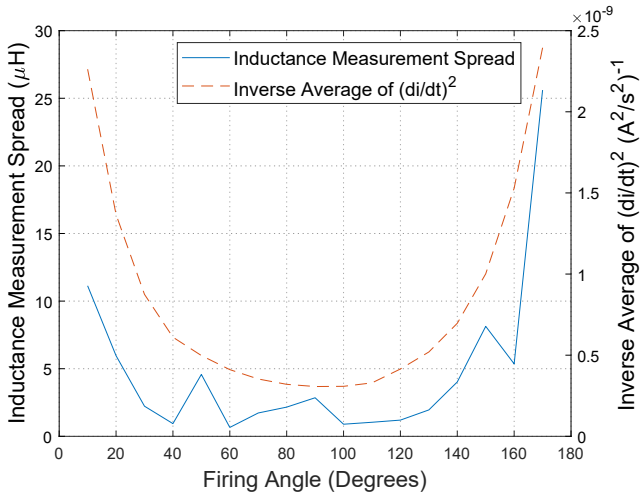


Fig. 15: Behavior of inductance values ranges measured with the added single-phase utility cable and the corresponding values of $< (\frac{di}{dt})^2 >^{-1}$.

for zero offset. Offset in the voltage probe does not matter since the "lambda method" works on differences in voltage measurements, not absolute voltage measurements.

The error in the inductance estimate for turn-on times near zero-crossings can be further explored by examining Eq. 1. In effect, the least-squares estimation method is attempting to find which values of $R$ and $L$ that best solve this equation for all data points. As shown in Fig. 14, as the firing angle approaches an integer multiple of 180°, the initial current inrush becomes smaller in comparison to peak inrush near 90°. At the extreme of a zero-crossing turn-on, the incandescent lamp has no sharp transient currents. The inrush becomes a slow transient on the order of a few milliseconds. Taking the time derivative of the current in this case only provides values near zero, but the overall magnitude of the current during the turn-on transient does not change significantly. That is, the data is insufficiently rich to support the two-parameter identification when taken close to zero crossings of the line voltage.

When the amplitude of current dominates over the amplitude of the time derivative of the current, Eq. 1 acts as a resistance estimator. The value of $L$ has less effect on the overall equation and varies in order to solve the resistance equation as closely as possible. Thus, the range and average values of the $L$ estimate become unreliable. The level of current does not change significantly over the range of currents. The consistent importance of $R$ in Eq. 1 makes the estimate repeatable and the resulting resistance estimate is relatively flat across the range. The small variation is expected as the equation changes to better fit a resistance value to the data.

To illustrate the effect of smaller average current time derivatives, Fig. 15 plots the the inverse average of the time derivative squared or $< (\frac{di}{dt})^2 >^{-1}$ along with the width of the inductance measurement variation. This time derivative measure is low for loads that have large amounts of $\frac{di}{dt}$ information and vice versa. A higher value of this measure correlates with less information about the inductance and thus a larger spread of inductance estimates. This figure provides a visual demonstration of this phenomenon and the limitation of using the "lambda method" with an arbitrary load to perform

line impedance estimation. To obtain better results, we could: (1) crop out data with low $\frac{di}{dt}$ to increase the average amount of useful information for the inductance estimate (2) use capacitors as a load as the ringing will interact heavily with the line inductance as used in [12]–[14] (3) use switching to increase the number of current steps possible as a TRIAC can only generate one step per half cycle. This last option becomes possible with a new version of the load switch implemented with MOSFETs which will be explored in future work.

## V. Conclusion

Inrush current testing is essential for many design, monitoring, and fault detection applications. Conventional AC source test equipment may not provide adequate capability for accurate inrush testing in real-world environments. This paper presents a circuit design for an inrush test device that can be applied on real-world source connections. The device is portable, flexible in its transient timing, rugged, and comparatively inexpensive compared to more general source devices that may offer less realistic power delivery constraints for practical testing. To illustrate the utility of the phase-controlled switch, this paper compares commercial AC source tests with data from the proposed device. The utility for other applications, especially *in situ* line impedance testing, was also presented. Testing can be conducted in a specific application environment. The phase-controlled switch can therefore be used to collect transient data for all sorts of applications, including power system monitoring and diagnostic testing.

All of these applications of the phase-controlled switch could potentially be expanded with other switch designs. A FET-based switch will offer the possibility of more complex test patterns within a single line cycle. More complex patterns offer interesting possibilities for more advanced system identification and impedance measurement.

## References


[1] L. Xue, X. Han, and S. Li, "Analysis of magnetizing inrush characteristics of electrified railway and its influence on grid voltage," in *2018 2nd IEEE Conference on Energy Internet and Energy System Integration (EI2)*, Oct 2018, pp. 1–6.

[2] M. Lacroix, P. Taillefer, and A. Mercier, "Mitigation of transformer inrush current associated with der facilities connected on the distribution grid," in *2015 IEEE Eindhoven PowerTech*, June 2015, pp. 1–5.

[3] R. Hamilton, "Analysis of transformer inrush current and comparison of harmonic restraint methods in transformer protection," *IEEE Transactions on Industry Applications*, vol. 49, no. 4, pp. 1890–1899, July 2013.

[4] Y. Z. Zhang and C. M. Bush, "Analysis and mitigation of interaction between transformer inrush current and hvdc operation," in *2017 IEEE Power Energy Society General Meeting*, July 2017, pp. 1–5.

[5] M. Demir, G. Kahramanoğlu, and A. Bekir Yıldız, "Importance of reliability for power electronic circuits, case study: Inrush current test and calculating of fuse melting point," in *2016 IEEE International Power Electronics and Motion Control Conference (PEMC)*, Sep. 2016, pp. 830–834.

[6] S. B. Leeb, "A conjoint pattern recognition approach to nonintrusive load monitoring," Ph.D. dissertation, Massachusetts Institute of Technology, 1993.

[7] M. Basseville and A. Benveniste, *Detection of Abrupt Changes in Signals and Dynamical Systems*. Springer, 1980.

[8] S. B. Leeb, S. R. Shaw, and J. L. Kirtley, "Transient event detection in spectral envelope estimates for nonintrusive load monitoring," in *IEEE Transactions on Power Delivery*, vol. 10, July 1995, pp. 1200–1210.

[9] D. Green, S. Shaw, P. Lindahl, T. Kane, J. Donnal, and S. Leeb, "A multi-scale framework for nonintrusive load identification," in *IEEE Transactions on Indusutrial Informatics*, June 2019.

[10] B. Griffith. How to measure inrush ac current. [Online]. Available: https://community.keysight.com/community/keysight-blogs/general-electronics-measurement/blog/2018/05/23/how-to-measure-inrush-ac-current

[11] Pacific Power. Peak current surge/inrush measurement programmable phase angle execution for the upc-1/3 programmable controller. [Online]. Available: http://pacificpower.com/Resources/Documents/DS4PEACKCURRENT092012.pdf

[12] W. Beattie and S. Matthews, "Impedance measurement on distribution networks," in *Proceedings of the 29th Universities Power Engineering Conference*, September 1994, pp. 117–120.

[13] S. Shaw, R. Lepard, , and S. Leeb, "Desire: A power quality prediction system," *28th Annual North American Power Symposium*, pp. 581–586, November 1996.

[14] S. R. Shaw, C. R. Laughman, S. B. Leeb, and R. F. Lepard, "A power quality prediction system," *IEEE Transactions on Industrial Electronics*, vol. 47, no. 3, pp. 511–517, June 2000.

[15] R. Johansson, *System Modeling and Identification*. Prentice-Hall, Inc., 1993.